1 **Codigestion of sludge and citrus peel wastes: Evaluating the**

2 **effect of biochar addition on microbial communities**

3 E.J. Martínez[a], J.G. Rosas[b], A. Sotres[a], A, Morán, J. Cara[a], M.E. Sánchez[a], X.

4 Gómez[a]*

5 [a]Chemical and Environmental Bioprocess Engineering Group, Natural Resources Institute (IRENA),
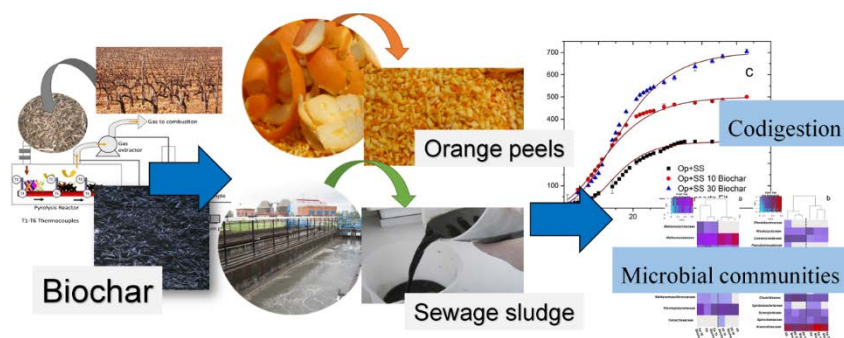
6 University of León, Av. de Portugal 41, 24009, Leon, Spain

7 [b]Department of electric engineering, School of Industrial Engineering and Informatics, University of

8 León, Campus de Vegazana, 24009, León, Spain.

9 *Correspondence to: Xiomar Gomez, Chemical and Environmental Bioprocess*

10 *Engineering Department, Natural Resources Institute (IRENA), University of León,*

11 *Avda de Portugal nº 41, León 24071, Spain. *E-mail of the corresponding author:*

12 *xagomb@unileon.es Telephone number: +34 987 29 5349*

13 ORCID number and E-mail of the first author E.J. Martínez: 0000-0002-4426-4353,

14 ejmartr@unileon.es

15 *E.J. Martínez and X. Gómez designed the experiment. E.J. Martínez, J.G. Rosas and A. Sotres*

16 *carried out the experiment. X. Gómez, J. Cara, M.E. Sánchez, E.J. Martínez and A. Sotres*

17 *prepared and revised the manuscript.*

18

19 **Codigestion of sludge and citrus peel wastes: Evaluating the**

20 **effect of biochar addition on microbial communities**

21 E. Judith Martínez[a], Jose Guillermo Rosas[b], Ana Sotres[a], Antonio Moran, Jorge Cara[a],

22 Marta Elena Sánchez[a], Xiomar Gómez[a]*

23 [a]Chemical and Environmental Bioprocess Engineering Group, Natural Resources Institute

24 (IRENA), University of León, Av. de Portugal 41, 24009, Leon, Spain

25 [b]Department of electric engineering, School of Industrial Engineering and Informatics,

26 University of León, Campus de Vegazana, 24009, León, Spain.

27 *E-mail of the corresponding author: xagomb@unileon.es Telephone number: +34 987 29

28 5349*

29 **Abstract**

30 In this study, the effects on process performance and changes in microbial populations

31 with the addition of biochar to the anaerobic digestion of sludge and orange peels were

32 evaluated. Biochar had a positive influence in batch digestions, leading to a decrease in

33 the lag phase and an increase in methane yields; this was even more evident for citrus

34 peel wastes, which reached an increase of approximately 33% when 10 g L^{-1} of biochar

35 was added and 56% when 30 g L^{-1} was added. Particle size analysis performed for the

AD	*Anaerobic digestion*
SS	*Sewage sludge*
CEO	*Citrus essential oil*
q_e	*Adsorption capacity*
PCR	*Polymerase chain reaction*
OTUs	*Operational Taxonomic Units*
PCA	*Principal components analysis*
DIET	*Direct interspecies electrons transfer*
SSA	*Specific surface area*
PSD	*Particle size distribution*
SMP	*Specific Methane potential*

36   experiments shows greater surface area available in biochar systems for biomass

37   immobilization.

38   Analysis of the microbial communities by means of *16S rRNA gene* pyrosequencing

39   shows that the biochar addition favoured the electro-active microorganisms consortia

40   creating a synthrophic metabolism between eubacterial and archaeal populations, which

41   resulted in an improvement of the anaerobic digestion performance.

42   The codigestion of the mixture under a semicontinuous regimen showed an

43   improvement in methane yields of approximately 60% and at hydraulic retention times

44   of 30–20 days (reaching methane production values above 500 L CH4 kg VS^{-1} at an

45   OLR of 1.49 kg VS m^{-3} d^{-1}). The enhancement observe in biochar supplemented

46   fermentations may be explained by the adsorption of inhibitors and the relatively high

47   surface area favoured the adhesion and growth of microorganisms.

1. Introduction

51   Biowastes can be transformed into useful resources through anaerobic digestion (AD),

52   which is an attractive technology for achieving pollution control and the recovery of

53   energy. Nevertheless, AD is a complex process where the intrinsic characteristics of

54   substrates, the presence of inhibitors and the reactor configuration are closely related to

55   the stability of the process. Consequently, different approaches have been applied to

56   attain higher benefits in terms of energy production and material recovery. These

57   approaches include codigestion, pretreatment of substrates, improvement of the reactor

58 configuration and the use of additives for reducing the effect of inhibitors and

59 increasing microbial activity.

60 AD is an effective technology widely applied for the treatment of sewage sludge (SS),

61 although several disadvantages such as low methane production and biodegradability

62 are well known [1,2]. This technology is usually optimized in many wastewater

63 treatment plants (WWTPs) by adding a cosubstrate or applying pretreatment strategies

64 to improve biogas yield and balance energy demands [3].

65 Valorization of citrus peel waste as a cosubstrate may represent an important source of

66 income for the food industry and to provide a new insight into waste management and

67 production of high-value products [4] . However, codigestion of this material also

68 requires the prior removal of inhibitory compounds, which would result in increased

69 treatment costs. Nearby, 50–60% of the total mass of the oranges consumed becomes

70 citrus peel waste, which is mainly composed of membranes, seeds and peels [5,6]. Due

71 to their main characteristics, the biological alternatives for their treatment such as

72 composting or ethanol fermentation are not always successful [7]. These characteristics

73 include a low pH of approximately 3–4, high water and organic matter contents, and the

74 presence of limonene, the main compound of citrus essential oils (CEO).

75 Limonene, which is a cyclic terpene, is the main compound present in CEO, with a

76 complex chemical structure (cyclohexane ring and ethylene group), making it resistant

77 to hydrolysis. Several studies have reported on its negative effects, which can severely

78 affect hydrolytic–acidogenic and methanogenic activity [6]. The concentration

79 thresholds reported for inhibitory effects show a wide range of values (24–192 CEO mg

80 $L^{-1}d^{-1}$). This high variability may be explained by the different conditions tested in their

81 experiments and the type of substrates used [5,6,8].

82   Different approaches have been used for improving the AD of citrus wastes, e.g.,

83   microbial acclimation or codigestion with other feedstocks in an attempt to reduce its

84   toxic effect [7,9]. However, the removal of limonene by different mechanisms (e.g.,

85   steam distillation, solvent extraction or adsorbents) is more effective because this

86   removal avoids further accumulation of limonene metabolites derived from microbial

87   activity, which may also act as inhibitors [5,8].

88   The use of low cost adsorbents such as biochar may become a feasible solution to avoid

89   inhibitory conditions. In addition, it should be borne in mind that biochar is frequently

90   produced from agro-industrial wastes; as such, this approach for preventing inhibition in

91   AD results in a holistic valorisation, thus allowing the integration of biological and

92   thermal processes with the aim of producing higher added value products, achieving

93   simultaneously environmental solutions and reducing the carbon footprint of industrial

94   processes. The integration of AD and thermal conversion processes as it is the case of

95   pyrolysis, results in higher energy gains, opening up new interesting pathways for the

96   valorisation of residual biomass. The integration of these two processes allows for the

97   use of pyrolysis by-products which can be easily integrated in the same valorisation unit

98   leading to a significant reduction of the organic material needing final disposal [10].

99   Although thermal processes may be seemed as expensive technologies due to their high

100   energy demand, pyrolysis has demonstrated capable of energy self- sufficiency

101   implying that no extra fuel is necessary for the operation of this type of technology

102   [11,12].

103

104   The addition of biochar to AD reduces the negative effects of toxic compounds and

105   promotes the immobilization of microbial biomass, due to the microporous structure.

106 Even though the mechanism of adsorption in biological systems has not been fully

107 studied, several authors have reported on the conjunction of adsorption and

108 immobilization for explaining the enhancements observed [13,14].

109 Mumme et al. [15] reported on the positive effects of biochar in avoiding the toxicity

110 caused by ammonia and others compounds. Similarly, Fagbohungbe et al. [8] reported

111 on the benefits for treating citrus peel wastes. It is well known that biochar provides a

112 relatively high surface area which favours the formation of biofilm and presents

113 conductive characteristics which may favour biological activity [16]. However, the

114 effect of these features on anaerobic microbial communities is still poorly understood,

115 particularly if special attention is to be payed to biochar–microbe interactions.

116 The aim of this study was to assess the influence of biochar addition on the anaerobic

117 codigestion of orange peels and sewage sludge. Bearing in mind the possible

118 mechanisms of improvement via adsorption and/or biomass immobilization, the process

119 was evaluated in terms of microbial populations, methane production and changes in the

120 main parameters such as volatile fatty acids, limonene, polyphenols, ammonia and

121 particle size.

122 The experiments were carried out in the Chemical and Environmental Bioprocess

123 Engineering Group at University of Leon during the years 2016 – 2017.

124 **2. Materials and methods**

125 *2.1 Characteristics of the substrates and biochar*

126 Sewage sludge (SS) and digested sludge (used as inoculum) were obtained from the

127 WWTP of the city of León, Spain. The total solids (TS) and volatile solids (VS)

128 contents of the inoculum were 35.5 ± 0.2 and 20.9 ± 0.2 g kg^{-1}, respectively. Sewage

129 sludge (SS) was stored at 4 ℃ prior to its further use. Orange peels (Op) were manually

130 chopped to obtain a particle size of 2–5 mm. No pretreatment was applied prior to

131 digestion. The physical and chemical characteristics of the Op are shown in Table 1.

132 **Table 1.HERE**

133 Biochar was produced from vineyard prunings from a vineyard in Barcelona, Spain.

134 The production of biochar was performed in a semi–continuous electrically heated

135 reactor. A full description of the process can be found elsewhere [17]. The biochar was

136 initially obtained using an electrical unit in order to develop an alternative management

137 of vineyards' residues from a Spanish winery. The aim was obtaining data for the

138 design and development of an energy self-sufficient pyrolysis plant which would aid in

139 the reduction of greenhouse gas emissions by biochar application to vineyards. The

140 main characteristics of the substrates and biochar are shown in Table 1.

141 *2.2 Adsorption experiments*

142 Adsorption experiments were carried out to evaluate the adsorption capacity of biochar.

143 The experiments were run using 250 mL Erlenmeyer flasks provided by magnetic

144 stirrers. The flasks contained 10 g L^{-1} of biochar and 100 mL of different solutions

145 containing acetic, propionic and butyric acid. Two replicates were tested for each

146 experiment. The solutions were prepared with a concentration range of 1 000−9 000 mg

147 L^{-1} for acetic, between 400 and 3 000 mg L^{-1} for propionic and from 400 to 4 000 mg L^{-}

148 ^{1} for butyric acid. The temperature was set at 25 ℃, and the initial pH was 7.0. The

149 initial and final concentrations were measured, and the data obtained were used to

150 calculate the adsorption capacity (qe) of the biochar and the removal achieved for each

151 compound (expressed in %). The results were fitted to a pseudo-second order model,

152 and adsorption kinetics constants were calculated based on the work of Martínez et

153 al.[18].

154 Initial concentrations against residual adsorbate concentration in the equilibrium were

155 fitted to the isothermal models of Langmuir and Freundlich. The Langmuir sorption

156 isotherm describes the sorption process at specific homogenous sites within the

157 adsorbent, assuming that the maximum adsorption corresponds to a monolayer saturated

158 with adsorbate molecules [18], Eq. (1):

159 $q_e = (Q * K_L * C_e) / (1 + K_L * C_e)$ (1)

160 where Q is a constant related to the adsorptive capacity, Ce is the equilibrium

161 concentration and K_L is a parameter of the adsorption energy.

162 The Freundlich isotherm is an empirical model and suggests that sorption energy

163 exponentially decreases upon occupation of the sorption site by an adsorbent, Eq. (2):

164 $q_e = K_F * C_e^{1/n}$ (2)

165 where K_F is a parameter related to the adsorption capacity and n refers to the process

166 intensity.

167 **2.3 Experimental set–up of anaerobic digestion**

168 *2.3.1 Batch test*

169 Batch digestion of the individual substrates, Op or SS, and of a mixture of the two at a

170 VS ratio of 1:1 (Op:SS) was tested (setting three replicates) using Erlenmeyer flasks of

171 250 mL. The flasks were filled with inoculum and substrate also at a VS ratio of 1:1

172 (inoculum-substrate, I:S). Sodium bicarbonate was added as a buffer against pH

173   changes, at a concentration of 10 g L^{-1}. Reactors containing inoculum were used as

174   blanks to subtract the background gas production. Temperature was controlled by a

175   water bath at 37 ± 1 °C, and agitation was provided by magnetic stirrers. Gas volumes

176   were measured using bottle gasometers and corrected to standard temperature and

177   pressure (STP, 0 ºC and 760 mmHg). Digestion systems were denoted as Op when

178   digesting orange peels, SS for sewage sludge and Op+SS for the mixture. Reactors

179   containing char were denoted Op+SS 10 Biochar and Op+SS 30 Biochar based on the

180   biochar content tested. Systems without substrate but containing the same amount of

181   char were also tested in order to observe if char itself promotes biogas production.

182   Methane production was fitted to the modified Gompertz equation [19]:

183    $$P_{(t)} = P1 + P_{max} \cdot \exp[- \exp(R_{max} \cdot e/P_{max})(\lambda - t) + 1]$$

184   where $P_{(t)}$ is the cumulative methane yield (L kg VS^{-1}), P_{max} is the maximum methane

185   yield (L kg VS^{-1}), R_{max} is the maximum methane production rate (L kg VS^{-1} d^{-1}), λ is the

186   lag–phase time (d) and e is Euler's number (approx. 2.718).

187   Data analysis was performed using OriginPro software. A modification to the model

188   was proposed when an extended lag phase was observed [19]. This modification

189   considers the addition of a new parameter corresponding to the initial methane

190   production obtained from the experiment (P1).

191   *2.3.2 Semicontinuous digestion*

192   Semicontinuous digestion was performed in completely stirred reactors (working

193   volume of 3 L) equipped with mechanical stirrers and outer-jackets to circulate heating

194   water at a temperature of 37 ± 1 °C. Feeding was manually performed once a day every

195   day. The start-up of the reactors was done using SS as substrate at a hydraulic retention

196   time (HRT) of 30 days for 15 days to allow for a progressive adaptation. Afterwards,

197   they were fed with the mixture of Op and SS. The organic loading rate (OLR) was

198   increased by reducing the HRT from 30 to 20 to 10 days subsequently. Biochar was

199   added to the reactor with the beginning of each HRT to reach a content of 10 g L^{-1}. The

200   biochar concentration in this reactor was calculated based on the following expression:

201
$$C_f = C_i\, e^{-\frac{1}{HRT}t}$$

202   where C_f is the biochar concentration (g L^{-1}) at the time t and C_i is the initial biochar

203   concentration (g L^{-1}).

204   The reactor denoted RC_Op+SS stands for the control system treating the mixture of Op

205   and SS. The reactor denoted RB_Op+SS represents the system treating the mixture with

206   the addition of biochar.

207   *2.4 Analytical techniques*

208   For liquid samples, ammonia, chemical oxygen demand (COD), TS, VS, pH, and

209   alkalinity were measured in accordance with APHA Standard Methods [20]. Total

210   organic carbon (TOC) and total nitrogen (TN) were measured for 25 ml of the

211   supernatant of centrifuged liquid sample (5000 rpm – 4193 x g, time of 5 min) using the

212   Analytik Jena Multi N/C_3100 system by thermocatalytic oxidation, Total carbon (TC)

213   and inorganic carbon (TIC) are determined separately. The difference results in TOC,

214   TOC = TC - TIC. The analysis of metals for the dried solid sample (0.3 g) was carried

215   out using a PerkinElmer Optima 2000 DV inductively coupled plasma (ICP) atomic

216   emission spectrometer as described in Fierro et al [21].

217   Biochar analysis was carried out using a LECO CHN-600 apparatus for measuring C,

218   H, and N in accordance with ASTM Standard D-5373. Ash content was determined

219   using a LECO MAC-300 thermogravimetric analyser (TGA). The Brunauer-Emmett-

220   Teller (BET) Surface Area method was performed with a Micromeritics model ASAP

221   2420 by adsorption isotherms of N_2 at 196 °C. Analysis of organic matter for substrates

222   (sewage sludge and orange peels) were measured by the use of the Walkley–Black

223   method [22]. TOC of substrates was calculated from the organic matter value, using a

224   correlation factor of 1.72.

225   D-Limonene was determined by bromate titration [23]. Total polyphenols (TP) were

226   measured by colourimetry at 760 nm on a Beckman DU640 spectrophotometer using

227   the Folin–Ciocalteau reagent in a mixture containing 650 µL of de-ionised water, 50 µL

228   of sample, 600 µL 7.5% Na_2CO_3 and 200 µL Folin–Ciocalteau reagent. Gallic acid was

229   used as standard for the calibration curve.

230   VFAs were measured by gas chromatography using a Varian CP3800 GC and a flame

231   ionisation detector equipped with a Nukol capillary column from Supelco. Biogas

232   composition was analysed using the same chromatograph when it was equipped with a

233   thermal conductivity detector. A packed column (HayeSep Q 80/100; 4 m) followed by

234   a molecular-sieve column (1 m) was used. The carrier gas was helium. Hydrogen

235   sulfide (H_2S) was detected using a pulse flame photometric detector (PFPD) with an

236   FA-II capillary column and helium as carrier gas.

237   Particle size analysis was performed using a Beckmann Coulter LS 13 320 laser

238   diffraction particle size analyser. The scatter generated was estimated based on the

239   Fraunhofer optical model. Samples were obtained from the SS batch digestion system.

240   Liquid samples were diluted in tap water prior to the analysis. Ten measurements were

241   performed for each sample.

242   *2.5 Microbial community analyses*

243   Samples for microbiological analysis were obtained from batch digestion tests and were

244   denoted following the nomenclature described previously for these tests: Op, Op 10

245   Biochar and Op 30 Biochar for the orange peel digestions, and SS, SS 10 Biochar and

246   SS 30 Biochar for the sewage sludge digestions. The sample denoted SS $_{Feed}$ contained

247   the sewage sludge that was used as substrate in the digestion systems.

248   Genomic DNA was extracted at the end of the batch experiments with the PowerSoil®

249   DNA Isolation Kit (MoBio Laboratories Inc., Carlsbad, CA, USA), following the

250   manufacturer's instructions. All PCR reactions were carried out in a Mastercycler

251   (Eppendorf, Hamburg, Germany), and PCR samples were checked for size of the

252   product on a 1% agarose gel.

253   The entire DNA extract was used for High Throughput Sequencing of *16S rRNA* gene

254   based massive libraries for eubacterial and archaeal communities. The primer set used

255   was 27Fmod (5`-AGRGTTTGATCMTGGCTCAG-3`) /519R modBio (5`-

256   GTNTTACNGCGGCKGCTG-3`) for the eubacterial population analysis and Arch

257   349F (5´- GYGCASCAGKCGMGAAW-3`) / Arch 806R

258   (5`GGACTACVSGGGTATCTAAT-3`) [24] for the archaeal population analysis. The

259   obtained DNA reads were compiled in FASTq files for further bioinformatics

260   processing following the procedure described by Sotres et al. (2016). Operational

261   Taxonomic Units (OTUs) were then taxonomically classified using the Ribosomal

262   Database Project (RDP) (https://rdp.cme.msu.edu/). The raw pyrosequencing data

263   obtained from this analysis were deposited in the Sequence Read Archive (SRA) of the

264   National Center for Biotechnology Information (NCBI), under nucleotide sequence

265   accession number SRP115155 for Eubacterial and Archaeal populations.

266   Microbial richness estimators (S_{obs} OTUs and *Chao1*) and diversity indices (*H'*, *inv*

267   *Simpson* and sampling *coverage*) were calculated using MOTHUR software, version

268   1.35.1, for each sample, after normalising the number of reads of all samples to those of

269   the sample with the lowest number of reads. Dynamics and similarity of the microbial

270   community structures were evaluated by principal components analysis (PCA) and

271   Venn diagrams based on the total of all OTUs obtained by high throughput sequencing.

272   The Venn diagram analysis was performed using VENNY software

273   (http://bioinfogp.cnb.csic.es/tools/venny/). Rstudio was used for performing PCA on the

274   OTU abundance matrix of both eubacterial and archaeal OTU populations, and it was

275   also used to produce heat maps.

276   **3. Results and discussion**

277   *3.1 Adsorption assays*

278   The adsorption experiments with organic acids (acetic, propionic and butyric) were

279   performed to obtain an approximation of the adsorption capacity of the biochar used

280   (q_e). The experimental value of q_e was 10.70 mg g^{-1} for acetic acid, 5.56 mg g^{-1} for

281   propionic acid and 3.15 mg g^{-1} for butyric acid, when the lower concentrations of the

282   organic acids were used (1000 mg L^{-1} of acetic, 400 mg L^{-1} of propionic and 400 mg L^{-1}

283   of butyric acid). In all of the cases, the adsorption capacity q_e increased with an increase

284   in the initial concentration. When the difference in concentrations was higher, the

285   driving force governing the process was also higher, favouring the mass transfer (data

286   are shown in supplementary material Fig. SM1 and Table SM1). The results were fitted

287   to the pseudo-second order model, and adsorption kinetics constants were calculated

288   based on this model. The calculated values of q_e were similar to the experimental data

289   obtained, indicating that the sorption systems belong to the pseudo-second order

290   kinetics model with regression coefficients higher than 0.95.

291   Different initial concentrations of VFAs (acetic, propionic and butyric) against residual

292   adsorbate concentration in the equilibrium were fitted to the isothermal models of

293   Langmuir and Freundlich. The values of the characteristic parameters obtained from the

294   fitting of both models (supplementary material Table SM2) indicated a better fit to the

295   Freundlich model for any of the VFA used (determination coefficients higher than

296   0.99). The *n* value (which is an indicator of the adsorption intensity) obtained for this

297   model was >1 for acetic acid, reflecting the favourable adsorption of this VFA. It has to

298   be noted that Freundlich parameters are only descriptive and unlike the Langmuir

299   model, it does not predict the formation of a boundary monolayer for adsorption,

300   showing a greater incorporation of the adsorbate.

301   The adsorption in water or in organic mixtures such as anaerobic digestion liquor is a

302   complex phenomenon due the differences in the adsorbent surfaces and specific

303   interactions of polar molecules with oxygen-containing surface groups [25]. Cuetos et al

304   [26] observed a mild retention of acids onto the activated carbon surface, which may

305   alleviated an inhibitory stage for microorganisms in the digestion of residual blood. The

306   adsorption capacity of biochar when used in digestion liquors may be affected since the

307   presence of a great variety of species may interfere and compete for adsorption sites.

308   *3.2 Batch digestion*

309   The cumulative methane production curves obtained from the different batch assays are

310   shown in Fig. 1. The fitted curves of the Gompertz model are also represented with

311   model parameters that are summarised in Table 2. No additional biogas production was

312   observed during the evaluation of the systems loaded only with char (data not shown).

313   **Fig. 1 HERE**

314   **Table 2. HERE**

315   The methane production curves presented a sigmoid profile showing an extended lag

316   phase when Op are digested, even with the addition of 10 g L^{-1} of biochar. This

317   behaviour is due to the need of acclimation of microorganism to the complex substrate

318   and high initial concentration of limonene (~600 mg L^{-1}).

319   The addition of biochar resulted in a reduction of the lag phase and a significant

320   increase in the methane production (see Table 2). Similarly, the assessment of biochar

321   addition on digestion of citrus peel wastes by Fagbohungbe et al. [8] revealed the

322   reduction of the lag phase from 13.4 to 6.8 days with wood biochar and a slight increase

323   of methane production with the addition of coconut shell biochar. Different methane

324   yields for orange peels and related biowastes have been reported in the literature, under

325   similar conditions of temperature but higher I:S ratio. Ruiz and Flotats [7] obtained an

326   average yield of 356 L CH_4 kg VS^{-1}, while Martin et al. (2010) reported 230 L CH_4 kg

327   VS^{-1} but in this case extracting limonene prior to digestion. Higher yield values have

328   been reported at thermophilic temperatures, around 400−600 L CH_4 kg VS^{-1} [27] In the

329   present study, the poor yield and extended lag phase reported for Op can be attributed to

330   the different operational parameters and higher limonene content.

331   The methane yields obtained from SS with and without the addition of biochar are

332   presented in Fig.1b. The process shows a small lag phase compared with that of the Op

333   system. The addition of biochar increased methane yield by approximately 33% when

334   10 g L^{-1} of biochar was added and by 56% when 30 g L^{-1} of biochar was added.

335   The results from the codigestion of Op and SS are shown in Fig. 1c. The methane yield

336   obtained from the Op+SS reactor was notably higher than that of the Op system (~89%)

337   and comparable to that of the SS reactor. This behaviour was explained by a dilution

338   effect caused by the way the feed was prepared and the type of the experimental set−up.

339   Reactors were initially loaded at a I:S ratio of 1:1, which was also the same for the

340   Op+SS mixture; therefore, the global amount of Op in the codigestion reactor was lower

341   than that of the Op digestion. The concentration of limonene when digesting the mixture

342   may have not reached inhibitory levels (336 against mg 620 L^{-1} in the Op reactor).

343   The benefits of biochar addition are evident from data reported in Table 2, when

344   treating the mixture Op+SS. The addition of biochar to the batch systems presents an

345   enhancement of the process, by increasing the gas production rate, improving yields or

346   decreasing the lag phase. These effects may be associated with the physical mechanisms

347   of adsorption of inhibitory compounds. In fact, the great improvement observed when

348   treating Op is related to the lower values of limonene and polyphenols measured (see

349   Fig. 2a−b). However, with regard to VFA, there is not a clear trend; the Op reactor

350   reached lower values during the first 10 days, with the exception of the particular low

351   concentration observed for butyric when biochar was added at its higher level. This may

352   be explained by the presence of a great diversity of compounds in the digestion liquor

353   which cause interference in the adsorption performance of biochar. Therefore, a lower

354   adsorption capacity of VFA was obtained in digestion tests, which was associated with

355   the presence of other counter-ions and compounds that may compete with organic acids

356   for adsorption sites.

357 **Fig. 2 HERE**

358 Fig. 2c also shows a rapid increase in VFA concentration regardless of whether or not

359 biochar had been added. Studies by Wang et al. [28] about the effects of VFA on

360 methane yield reported that acetic acid concentrations of 2 400 mg L^{-1} and butyric acid

361 concentrations of 1 800 mg L^{-1} may not cause a significant inhibition of the activity of

362 methanogens, while a propionic acid content of 900 mg L^{-1} could result in significant

363 inhibition. The digestion of Op resulted in a rapid degradation of the substrate leading to

364 VFA build-up, mainly of acetic acid (reaching ~12 000 mg L^{-1}) and butyric acid

365 (reaching~5 000 mg L^{-1}), to levels above inhibitory thresholds. Nonetheless, the

366 concentration at which VFAs can cause inhibition depends on the previous conditions,

367 hence the impossibility of defining VFA levels to indicate the state considered as

368 'normal' for the anaerobic process [29]. However, in the case of propionic acid, the

369 values for this system were initially much lower than those from reactors with biochar

370 addition. At the end, these later systems consumed this acid while the Op reactor

371 maintained an increasing trend reaching a final concentration of 2 100 mg L^{-1}, a much

372 higher value than that of biochar systems.

373 After 30 days of operation, the acetic and butyric acid concentrations decreased

374 significantly with biochar addition, with especially low values attained for butyric acid.

375 The final values of VFA for biochar containing reactors were 1 790 mg L^{-1} for Op 10

376 Biochar and 1 459 mg L^{-1} for Op 30 Biochar, indicating that although a better

377 assimilation of the organic material can be associated with the presence of biochar,

378 methanogenic microorganisms were not capable of consuming all VFAs derived from

379 the hydrolysis−acidification stages.

17

380   It may be reasonable to assume that the presence of limonene and polyphenols were

381   causing interference in the adsorption of VFA. Further work is necessary to elucidate

382   the effect of biochar on the adsorption of these compounds and their interaction with

383   VFA. The concentration of limonene and polyphenols was lower for biochar

384   supplemented systems at the end of the digestion tests (Fig. 2a – 2b), indicating that

385   there is an adsorption effect taking place for these two compounds and explaining the

386   different results in VFA adsorption tests of single acids and digestion tests

387   The evolution of VFA reported in Fig. 2c indicates that adsorption may not be playing a

388   crucial role on the enhancement obtained in methane yields when biochar was added,

389   since initial values of VFA were similar to those of the Op reactor. A mechanism that

390   has been suggested when using conductive carbon materials is the direct interspecies

391   electrons transfer (DIET), a syntrophic metabolism where free electrons flow from one

392   cell to another without being shuttled by reduced molecules such as molecular hydrogen

393   or formate [30]. This mechanism has been suggested as responsible for obtaining better

394   degradation rates of simple substrates and higher biogas yields in anaerobic systems

395   when conductive carbon materials are added [26].

396   An explanation behind the improvement of digestion may be gained from the behaviour

397   of the SS digestion set-up when studying the particle size distribution. In this case, the

398   presence of inhibitory substances lacks relevance, so the effect of adsorption of toxic

399   compounds is not considered. Modifications in the physical structures of aggregates

400   formed due to the addition of biochar may have caused an improvement in

401   microorganism consortia. Samples from the SS reactors were obtained at the end of the

402   digestion.

403   The particle size analysis performed for the SS digestion test shows the impact of

404   biochar addition in the main parameters measured. Table 3 summarizes the results

405   obtained at the end of the experiments. The value for specific surface area (SSA) was

406   33% higher for SS 10 Biochar and 47% for SS 30 Biochar samples when compared with

407   the SS digested sample.

408   **Table 3.HERE**

409   The particle size distribution (PSD) of biochar was centred between $1-1000$ µm of

410   particle size. The distribution shows three main peaks, one located between $40-400$

411   µm, one corresponding to small particles between $1-40$ µm and the other between

412     $400-1000$ µm. This sample had a mode of 185.4 µm particle size and an SSA of 2890

413     $cm^2 \, g^{-1}$ (see supplementary material Fig. SM2a).

414   The PSD shows a similar bimodal distribution for all SS samples after digestion. The

415   main peak is centred in the smaller particle range, with samples SS and SS 10 Biochar

416   presenting also a minor peak centred between $100-300$ µm (see supplementary material

417   Fig. SM2b). The major differences observed were associated with the values of SSA.

418   The greater surface area available in biochar systems may have favoured biomass

419   immobilization and assisted the microbial consortia in the access to substrate,

420   improving the assimilation of acid intermediaries and, as a consequence, methane

421   yields.

422   Similar experiments carried out by several authors using carbon additives in anaerobic

423   digestion also report on an improvement thanks to the influence of the supporting

424   material causing the selection of some microorganisms over others [13,14].

425   Watanabe et al. [31] demonstrated the improvement caused by the addition of cedar

426   charcoal when SS and crude glycerol were codigested. The better performance was

427   explained by the attachment on charcoal particles of microorganisms capable of

428   producing methane from glycerol.

429   *3.3 Microbial community structure*

430   The reads and the coverage values obtained for eubacterial and for archaeal

431   communities are shown in Tables SM3 and SM4 (see supplementary material). The

432   number of quality reads per sample ranged from 80 093 to 103 331 for eubacteria and

433   from 18 604 to 102 847 for archaea. The differences in species richness indicators (S_{obs}

434   OTUs and *Chao1* estimator) and diversity indices (*H'* and *1/Simpson*) are described in

435   Tables SM3 and SM4 (see supplementary material).

436   The PCA results for the eubacterial community can be seen in Fig. SM3a. The

437   microbial community on the Op and SS digestion was modified based on that obtained

438   from samples of the Inoculum and SS_{Feed}. The two anaerobic systems clustered together,

439   being separated from each other. In the Venn diagram, substantial differences in the

440   total of OTUs in the Op digestion system when biochar was added (Op 10 Biochar, Op

441   30 Biochar) are represented (see supplementary material Fig. SM3b). It is highlighted

442   that not a single OTU was shared between the Op sample and the samples obtained

443   when biochar was added (29.5% of the total OTUs were shared between Op 10 Biochar

444   and Op 30 Biochar). On the other hand, there are not such dramatic differences with the

445   SS digestion set-up, since 35.3% of the total OTUs were shared between the SS sample

446   and those with biochar added (SS 10 Biochar, SS 30 Biochar).

447   The PCA results for the archaeal community (see supplementary material Fig. SM4a)

448   were similar to those for the eubacterial community. Nevertheless, the Venn diagram

449   showed that biochar addition did not induce a dramatic shift on the total of observed

450   OTUs for the archaeal community with the Op digestion, since 245 OTUs, equivalent to

451   52.1% of the total OTUs were shared between Op, Op 10 Biochar and Op 30 Biochar

452   samples (see supplementary material Fig. SM4b). Similarly, 47.7% of the total OTUs

453   were common in the sludge set-up (SS, SS 10 Biochar and SS 30 Biochar samples). As

454   a result, biochar addition led the sharpest change in the eubacterial community of the

455   Op digestion.

456   The effect of biochar addition was studied by phylogenetic identification in the

457   eubacterial and archaeal communities. Heat maps at the family level (Fig. 3) for the

458   eubacterial and archaeal communities showed two clusters clearly differentiated for Op

459   and SS samples. Although no significant difference in family composition for the

460   archaeal community were observed (Fig. 3a), shifts in the relative abundance of some

461   families were noteworthy. When Op and Op 30 Biochar samples were compared, an

462   increase was observed in the relative abundance of *Methanomicrobiaceae* from 1.2% to

463   9.1%, *Methanosarcinaceae* from 3% to 5.4% and *Thermoplasmataceae* from 3.2% to

464   14.7%. On the other hand, slight differences were observed in the case of the SS

465   digestion experiment, increasing the abundance of three families by less than 2% when

466   30 g L^{-1} of biochar was added. *Methanobacteriaceae* and *Methanoregulaceae* and two

467   families *Methamassiliicoccaceae* and *Cenarchaeaceae* were identified only after

468   biochar addition.

469   **Fig. 3 HERE**

470   *Methanosaetaceae* was the dominant family found in samples obtained from Op and SS

471   experimental set-up, accounting for 41−49% (Op experiment) and 59−60.5% (SS

472   experiment) of the total archaeal community. *Methanosaetaceae* was initially

473   predominant in the SS_{Feed} (45%) and in the inoculum sample (43.1%) (data not shown).

474   Eubacterial communities at the family level were more sensitive than archaeal

475   communities to the biochar addition, as shown in Fig. 3b. In the Op system,

476   *Peptococcaceae* turned out to be the most affected family, being completely inhibited

477   after biochar addition. Some families were completely inhibited after biochar addition

478   in both Op and SS systems, such as *Symbiobacteriaceae* and *Peptococcaceae* (within

479   the phylum *Firmicutes*), and *Pseudomonadaceae* and *Rhodobacteraceae* (within the

480   phylum *Proteobacteria*).

481   The most abundant group in all samples was the family *Anaerolineaceae* (within the

482   phylum *Chloroflexi*), which performs syntrophically in cooperation with

483   *Methanosaetaceae*, also abundant in all samples as described above (Fig. 3a). Both

484   groups have been described to be the predominant microorganisms and to be involved

485   in the process of methanogenic degradation of alkanes [32]. The next most abundant

486   group, also present in all samples, was the family *Clostridiaceae*, which belongs to the

487   phylum *Firmicutes*.

488   Microbial community structure was also studied at the genus level (Fig. 4 and 5). The

489   results obtained for Op digestion revealed that 9 genera increased their relative

490   abundance after biochar addition, namely, *Bellilinea*, *Trepomena*, *Cythophaga*,

491   *Dechloromonas*, *Clostridium*, *Petrimonas*, *Proteiniphilum*, *Bacteroides* and

492   *Eubacterium*. In addition, 5 genera were identified only in Op 10 Biochar and Op 30

493   Biochar: *Spaerochaeta*, *Spirochaeta*, *Thermolithobacter*, *Petrotoga* and *Acidovorax*.

494   Although minor, some changes were also detected for the archaeal genera, with the

495   relative abundance of *Thermogymnomonas* and three hydrogenotrophic methanogens,

496 *Methanofollis*, *Methanoculleus* and *Methanolinea*, being increased. In addition,

497 *Methanobacterium* decreased in abundance after biochar addition.

498 **Fig. 4 HERE**

499 **Fig. 5 HERE**

500 In the SS digestion, changes were also detected in the relative abundance of some

501 genera. For the eubacterial community, the biochar addition had a positive effect on

502 *Clostridium*, *Curvibacter*, *Petrimonas*, *Eubacterium*, and *Syntrophomonas* genera. This

503 last genus, *Syntrophomonas*, is an anaerobic, syntrophic and fatty acid oxidizing

504 bacteria, previously described in anaerobic digestion works using biochar [14], and

505 additionally these bacteria participate in a methanogenic syntrophy with H_2 using

506 archaea such as *Methanospirillum* [33], also present in this study. *Geobacter* was

507 identified when biochar was added to the anaerobic digestion SS 30 Biochar but not at

508 the lower biochar level.

509 In the archaeal structure, only *Methanobacterium* and *Methanolinea*, both

510 hydrogenotrophic methanogens, slightly increased their relative abundance.

511 Another two important genera, *Clostridium* and *Geobacter*, were also detected in batch

512 experiments such for Op and SS digestion. *Clostridum* increased their abundance in

513 both anaerobic systems after the addition of Biochar, being the most abundant genus in

514 system SS 30 Biochar, accounting for 25% of the total population, and being the second

515 most abundant in Op 30 Biochar. *Clostridium* is known to be a homoacetogenic bacteria

516 and active fermenter, and a correlation between this genus and high methane production

517 has been previously described in the literature, which may signify a syntrophic

518 association with methanogens [34]. The well-known exoelectrogenic *Geobacter* was

519 one of the bacterial models used to study the conductive properties of biochar, and the

520   impact of these bacteria on direct electron transfer (DIET) [35], mainly with

521   *Methanosarcina* and *Methanosaeta,* was also evident in our experiments.

522   Even though differences in the eubacterial community populations were observed

523   between Op and SS anaerobic digestion, some bacteria were favoured under the biochar

524   influence in both systems. *Treponema* is a *Spirochaeta* also described together with

525   *Geobacter* in conductive biofilms [36], which also increased their abundance with

526   biochar addition, probably explaining its presence at the higher level tested (30 g L^{-1})

527   but not at the lower level. *Petrimonas* (in the family *Porphyromonadaceae*) have a

528   fermentative type metabolism, with the final fermentation products of glucose being

529   acetate, H_2 and CO_2. The genus *Dechloromonas* (belongs to the family

530   *Rhodocyclaceae*), are described as H_2 producing bacteria. Hence, it is likely that the

531   addition of biochar aids in the formation of co-cultures that produce H_2 or formate,

532   providing electrons for CO_2 reduction (to produce methane) by H_2 utilizing

533   methanogens, as *Methanolinea*, *Methanobacterium*, *Methanosarcina*,

534   *Methanomassiliicoccus*, and *Methanofollis,* which were favoured by the addition of

535   biochar, while the acetoclastic *Methanosaeta*, the most abundant group in both systems,

536   decreased their relative abundance.

537   ***3.4 Semicontinuous digestion***

538   The results of semicontinuous digestion are presented in Fig. 6(a−e) and Table 4. After

539   an adaptation period with sludge feeding, the reactors RC_Op+SS (control) and

540   RB_Op+SS (biochar addition) were fed in a semicontinuous mode with the mixture and

541   evaluated with a decreasing HRT. The biochar addition and concentration in the reactor

542   is reflected in Fig. 6b.

543   **Table 4. HERE**

544 A fluctuating process was observed for the codigestion system due to the presence of

545 limonene in the feed, which severely affected the microbial activity (Fig. 6c). Biochar

546 significantly improved the specific methane production (SMP) at the different HRTs

547 studied (30−20 days) ($P < 0.05$, one-way ANOVA, Tukey *post hoc* test) and also

548 attained a slight reduction in H_2S concentration in biogas along with lower levels of

549 VFA content (Table 4).

550 Ammonium content in both reactors was similar ($P > 0.05$, one-way ANOVA)

551 indicating that the addition of biochar had no effect on the evolution of this compound.

552 The sludge sample had an initial ammonium content of 678 ± 89 mg L^{-1}. The digestion

553 of sludge leads to the degradation of proteins releasing in consequence nitrogen in the

554 form of ammonium. Reactors presented ammonium values in the range of 1300 to 1800

555 mg L^{-1}. Since the organic co-substrate added does not present a high content of

556 nitrogen, its addition to the digester will not lead to ammonium inhibitory problems. In

557 the case of a hypothetical implementation of this type of co-digestion in a WWTP

558 accumulation of this compound in the water line due to the recycling of digestate

559 supernatant from sludge decanters should therefore not to be expected. In terms of

560 ammonium load, the use of this type of cosubstrate will not derive in the emergence of

561 additional environmental problems regarding sludge disposal.

562 Results were in accordance with the benefits associated with the adsorption of

563 inhibitory compounds like limonene and with the immobilisation of biomass. The

564 dramatic variability in methane production observed in this reactor during the initial

565 HRTs and the similar methane production achieved at an HRT of 10 days with that of

566 RC_Op+SS (Fig. 6a) can be attributed to the adsorption-desorption phenomena and

567 saturation of the added biochar, which resulted in the release of limonene into the bulk

568　　solution, thereby affecting the microbial activity. No significant changes were observed

569　　for the other parameters measured when evaluating the effect of biochar addition (Fig.

570　　6d−e). Nevertheless, under mesophilic conditions, the addition of biochar to attain a

571　　content in the range of $3-20$ g L^{-1} significantly improved the Op+SS system, reaching

572　　methane production values above 500 L CH_4 kg VS^{-1} at an OLR of 1.49 kg VS m^{-3} d^{-1},

573　　similar to the results from batch tests.

574　　**Fig. 6 HERE**

575　　The SMP obtained for both systems significantly decreased with the increase in OLR,

576　　from 1.49 to 4.48 kg VS m^{-3} d^{-1}. The performance of both reactors was quite similar at

577　　the end of the 20 d HRT, and this was also true with the further decrease to 10 d. The

578　　reloading of char on day 105 (its contents reached 15 g L^{-1}) was not sufficient and gas

579　　performance was initially affected. This behaviour was also followed by a decrement in

580　　other parameters (VFA build-up, limonene and polyphenols increments). Analogous

581　　experiments by different authors have suggested an inhibition of the process by high

582　　organic loading. The results of Serrano et al. [9] with SS and Op codigestion (70:30 wet

583　　weight respectively) showed a lower methane yield, 165 L CH_4 kg^{-1} VS, with an OLR

584　　being increased from 0.4 to 1.6 kg VS m^{-3} d^{-1}. The studies carried out by Martin et al.

585　　[5], also an Op digestion, presented a decrement in methane production with the

586　　increase in OLR for values above 3.5 g COD m^{-3} d^{-1}.

587　　**4.　Conclusions**

588　　The addition of biochar had a positive influence on the anaerobic digestion evaluated. In

589　　batch systems, a decrease in the lag phase and an increase in methane yields were

590　　observed. The benefits were more noticeable in systems with higher content of biochar

591   (30 g L^{-1}) and were more significant for the Op system which presented a greater

592   improvement in methane yield. ~~The digestion can be improved due to the conductive~~

593   ~~properties of biochar, which may aid in H$_2$/formate transfer between syntrophic~~

594   ~~microorganisms rather than the formation of aggregates directly connected between the~~

595   ~~microbes.~~

596   The microbial community composition shows differences in both SS and Op systems.

597   However, pyrosequencing analysis showed that biochar addition led to similar

598   populations shifts in both anaerobic digestion reactors, where biochar favoured the

599   electro-active microorganisms consortia creating a syntrophic metabolism through

600   conductive carbon materials. The most highlighted changes could be the enrichment of

601   well know homoacetogenic bacteria such as *Clostridium* and *Eubacterium*, *Geobacter*,

602   *Syntrophomonas* and *Anaerolineaceae*, which peform syntrophically with H$_2$ using

603   archaea and also with *Methanosaeta*. Therefore, the addition of biochar allowed the

604   formation of co-cultures that improved the production of methane and as a consequence,

605   the performance of anaerobic digestion. An enhancement on the average methane yield

606   was obtained for the codigestion of Op and SS under semicontinuous regimen. Higher

607   amounts of biochar would be necessary to maintain the stability of the process,

608   especially during substrate-induced inhibition. Biochar addition avoids system decay

609   due to its adsorption capacity for inhibitors.

6. References

[1] B.M. Cieślik, J. Namieśnik, P. Konieczka, Review of sewage sludge management: standards, regulations and analytical methods, J. Clean. Prod. 90 (2015) 1–15. doi:10.1016/j.jclepro.2014.11.031.

[2] F. Tufaner, Y. Avşar, Effects of co-substrate on biogas production from cattle manure: a review, Int. J. Environ. Sci. Technol. 13 (2016) 2303–2312. doi:10.1007/s13762-016-1069-1.

[3] X. Dai, X. Li, D. Zhang, Y. Chen, L. Dai, Simultaneous enhancement of methane production and methane content in biogas from waste activated sludge and perennial ryegrass anaerobic co-digestion: The effects of pH and C/N ratio, Bioresour. Technol. 216 (2016) 323–330. doi:10.1016/J.BIORTECH.2016.05.100.

[4] M.H. Haddadi, H.T. Aiyelabegan, B. Negahdari, Advanced biotechnology in biorefinery: a new insight into municipal waste management to the production of high-value products, Int. J. Environ. Sci. Technol. (2017). doi:10.1007/s13762-017-1424-x.

[5] M.A. Martin, J.A. Siles, A.F. Chica, A. Martin, Biomethanization of orange peel waste., Bioresour. Technol. 101 (2010) 8993–8999. doi:10.1016/j.biortech.2010.06.133.

[6] P.S. Calabrò, L. Pontoni, I. Porqueddu, R. Greco, F. Pirozzi, F. Malpei, Effect of

636 the concentration of essential oil on orange peel waste biomethanization:

637 Preliminary batch results, Waste Manag. 48 (2016) 440–447.

638 doi:10.1016/j.wasman.2015.10.032.

639 [7] B. Ruiz, X. Flotats, Effect of limonene on batch anaerobic digestion of citrus peel

640 waste, Biochem. Eng. J. 109 (2016) 9–18. doi:10.1016/j.bej.2015.12.011.

641 [8] M.O. Fagbohungbe, B.M.J. Herbert, L. Hurst, H. Li, S.Q. Usmani, K.T. Semple,

642 Impact of biochar on the anaerobic digestion of citrus peel waste, Bioresour.

643 Technol. 216 (2016) 142–149.

644 doi:http://dx.doi.org/10.1016/j.biortech.2016.04.106.

645 [9] A. Serrano, J.A. Siles López, A.F. Chica, M.A. Martín, F. Karouach, A.

646 Mesfioui, et al., Mesophilic anaerobic co-digestion of sewage sludge and orange

647 peel waste, Environ. Technol. 35 (2014) 898–906.

648 doi:10.1080/09593330.2013.855822.

649 [10] F. Monlau, M. Francavilla, C. Sambusiti, N. Antoniou, A. Solhy, A. Libutti, et

650 al., Toward a functional integration of anaerobic digestion and pyrolysis for a

651 sustainable resource management. Comparison between solid-digestate and its

652 derived pyrochar as soil amendment, Appl. Energy. 169 (2016) 652–662.

653 doi:10.1016/j.apenergy.2016.02.084.

654 [11] H. Cong, O. Mašek, L. Zhao, Z. Yao, H. Meng, E. Hu, et al., Slow Pyrolysis

655 Performance and Energy Balance of Corn Stover in Continuous Pyrolysis-Based

656 Poly-Generation Systems, Energy & Fuels. 32 (2018) 3743–3750.

657 doi:10.1021/acs.energyfuels.7b03175.

658 [12] Z. Wang, D. Chen, X. Song, L. Zhao, Study on the combined sewage sludge

659   pyrolysis and gasification process: mass and energy balance, Environ. Technol.

660   33 (2012) 2481–2488. doi:10.1080/09593330.2012.683816.

661   [13]   F. Lü, C. Luo, L. Shao, P. He, Biochar alleviates combined stress of ammonium

662   and acids by firstly enriching Methanosaeta and then Methanosarcina, Water Res.

663   90 (2016) 34–43. doi:10.1016/j.watres.2015.12.029.

664   [14]   C. Luo, F. Lü, L. Shao, P. He, Application of eco-compatible biochar in

665   anaerobic digestion to relieve acid stress and promote the selective colonization

666   of functional microbes, Water Res. 68 (2015) 710–718.

667   doi:10.1016/j.watres.2014.10.052.

668   [15]   J. Mumme, F. Srocke, K. Heeg, M. Werner, Use of biochars in anaerobic

669   digestion, Bioresour. Technol. 164 (2014) 189–197.

670   doi:10.1016/j.biortech.2014.05.008.

671   [16]   A. Prévoteau, F. Ronsse, I. Cid, P. Boeckx, K. Rabaey, The electron donating

672   capacity of biochar is dramatically underestimated, Sci. Rep. 6 (2016).

673   doi:10.1038/srep32870.

674   [17]   J.G. Rosas, N. Gómez, J. Cara, J. Ubalde, X. Sort, M.E. Sánchez, Assessment of

675   sustainable biochar production for carbon abatement from vineyard residues, J.

676   Anal. Appl. Pyrolysis. 113 (2015) 239–247. doi:10.1016/j.jaap.2015.01.011.

677   [18]   E.J. Martínez, J. Fierro, J.G. Rosas, A. Lobato, M. Otero, X. Gómez, Assessment

678   of cationic dye biosorption onto anaerobic digested sludge: Spectroscopic

679   characterization, Environ. Prog. Sustain. Energy. 35 (2016).

680   doi:10.1002/ep.12352.

681   [19] C. Fernández, B. Carracedo, E.J. Martínez, X. Gómez, A. Morán, Application of

682   a packed bed reactor for the production of hydrogen from cheese whey permeate:

683   Effect of organic loading rate, J. Environ. Sci. Heal. - Part A Toxic/Hazardous

684   Subst. Environ. Eng. 49 (2014). doi:10.1080/10934529.2013.838885.

685   [20] APHA, AWWA, WEF, Standard Methods for the Examination of Water and

686   Wastewater, 1999.

687   [21] J. Fierro, E.J. Martinez, J.G. Rosas, R.A. Fernández, R. López, X. Gomez, Co-

688   Digestion of Swine Manure and Crude Glycerine: Increasing Glycerine Ratio

689   Results in Preferential Degradation of Labile Compounds, Water, Air, Soil

690   Pollut. (2016).

691   [22] A. Walkley, I.A. Black, An examination of the Degtjareff method for

692   determining soil organic matter, and a proposed modification of the chromic acid

693   titration method., Soil Sci. 37 (1934) 29–38.

694   [23] W.C. Scott, M.K. Veldhuis, Rapid estimation of recoverable oil in citrus juices

695   by bromate titration, J. Assoc. Off. Anal. Chem. 49 (1966) 628.

696   [24] A. Sotres, L. Tey, A. Bonmatí, M. Viñas, Microbial community dynamics in

697   continuous microbial fuel cells fed with synthetic wastewater and pig slurry,

698   Bioelectrochemistry. 111 (2016) 70–82.

699   doi:10.1016/J.BIOELECHEM.2016.04.007.

700   [25] V.V. Turov, V.M. Gun'ko, R. Leboda, T.J. Bandosz, J. Skubiszewska-Zieba, D.

701   Palijczuk, et al., Influence of Organics on the Structure of Water Adsorbed on

702   Activated Carbons, J. Colloid Interface Sci. 253 (2002) 23–34.

703   doi:10.1006/JCIS.2002.8547.

704   [26]   M.J. Cuetos, E.J. Martinez, R. Moreno, R. Gonzalez, M. Otero, X. Gomez,

705   Enhancing anaerobic digestion of poultry blood using activated carbon, J. Adv.

706   Res. 8 (2017) 297–307. doi:10.1016/j.jare.2016.12.004.

707   [27]   P.L.N. Kaparaju, J. a Rintala, Thermophilic anaerobic digestion of industrial

708   orange waste., Environ. Technol. 27 (2006) 623–633.

709   doi:10.1080/09593332708618676.

710   [28]   Y. Wang, Y. Zhang, J. Wang, L. Meng, Effects of volatile fatty acid

711   concentrations on methane yield and methanogenic bacteria, Biomass and

712   Bioenergy. 33 (2009) 848–853. doi:10.1016/j.biombioe.2009.01.007.

713   [29]   I.H. Franke-Whittle, A. Walter, C. Ebner, H. Insam, Investigation into the effect

714   of high concentrations of volatile fatty acids in anaerobic digestion on

715   methanogenic communities, Waste Manag. 34 (2014) 2080–2089.

716   doi:10.1016/j.wasman.2014.07.020.

717   [30]   C.D. Dubé, S.R. Guiot, Direct interspecies electron transfer in anaerobic

718   digestion: A review, in: Biogas Sci. Technol., 2015: pp. 101–115.

719   doi:10.1007/978-3-319-21993-6_4.

720   [31]   R. Watanabe, C. Tada, Y. Baba, Y. Fukuda, Y. Nakai, Enhancing methane

721   production during the anaerobic digestion of crude glycerol using Japanese cedar

722   charcoal, Bioresour. Technol. 150 (2013) 387–392.

723   doi:10.1016/j.biortech.2013.10.030.

724   [32]   B. Liang, L.-Y. Wang, S.M. Mbadinga, J.-F. Liu, S.-Z. Yang, J.-D. Gu, et al.,

725   Anaerolineaceae and Methanosaeta turned to be the dominant microorganisms in

726   alkanes-dependent methanogenic culture after long-term of incubation., AMB

727   Expr. 5 (2015) 37. doi:10.1186/s13568-015-0117-4.

728   [33]   D.R. Boone, R.L. Johnson, Y. Liu, Diffusion of the Interspecies Electron Carriers

729   H2 and Formate in Methanogenic Ecosystems and Its Implications in the

730   Measurement of Km for H2 or Formate Uptake, Appl. Environ. Microbiol. 55

731   (1989) 1735–1741. doi:0099-2240/89/071735-07$02.00/0.

732   [34]   I. Vanwonterghem, P.D. Jensen, D.P. Ho, D.J. Batstone, G.W. Tyson, Linking

733   microbial community structure, interactions and function in anaerobic digesters

734   using new molecular techniques, Curr. Opin. Biotechnol. 27 (2014) 55–64.

735   doi:10.1016/j.copbio.2013.11.004.

736   [35]   F. Liu, S. Chen, A.-E. Rotaru, P.M. Shrestha, N.S. Malvankar, W. Fan, et al.,

737   Promoting interspecies electron transfer with activated carbon, Sci. Rep. 4 (2014)

738   5019. doi:10.1038/srep05019.

739   [36]   B.R. Dhar, H. Ryu, J.W. Santo Domingo, H.-S. Lee, Ohmic resistance affects

740   microbial community and electrochemical kinetics in a multi-anode microbial

741   electrochemical cell, J. Power Sources. 331 (2016) 315–321.

742   doi:10.1016/j.jpowsour.2016.09.055.

743

744

745

746

747 **Table 1.** Substrates and Biochar characterisation

Parameters	Op	SS	Parameters	Biochar
pH	5.15±0.05	5.66±0.05	Moisture (wt.%)	1.59±0.60
COD $_{soluble}$ (mg L^{-1})	23000±460	3869±193	Volatile matter [a] (wt.%)	21.0±2.0
TOC $_{soluble}$ (%)	43.72±0.5	34.69±0.5	Ash[a] (wt.%)	47.4±1.8
VFA (mg L^{-1})	70±4	2602±169	Fixed carbon[a,c] (wt.%)	31.6±3.8
TS (g kg^{-1})	311±37	28.7±0.6	C[b] (wt.%)	74.5±5.3
VS (g kg^{-1})	302±35	23.28±0.5	N[b] (wt.%)	0.7±0.2
Ammonia (mg L^{-1})	n.m	687±89	H[b] (wt.%)	1.51±0.24
Organic matter (%)[a]	75.2	59.68	S[b] (wt.%)	0.05±0.04
N Kjeldahl (%)[a]	0.82	7.34	O[b,c] (wt.%)	23.27±5.39
C/N	53.3	4.72	O/C	0.2
Cu (mg kg^{-1})	4.61±0.04	3.32±0.02	H/C	0.24±0.01
Zn (mg kg^{-1})	5.34±0.10	19.61±0.25	HHV (MJ kg^{-1})	12.89 ±1.84
P (mg kg^{-1})	601±6	681.06±13.29	S$_{BET}$ isotherm. N$_2$ (m^2 g^{-1})	240±4.8

748   Chemical oxygen demand (COD), total organic carbon (TOC), volatile fatty acids (VFA),

749   higher heating value (HHV), surface area (S$_{BET}$ isotherm. N$_2$), n.m.: not measured.

750   [a] in a dry matter basis; [b] in a dry ash free basis; [c] Calculated by difference.

751

752 **Table 2.** Kinetic Gompertz parameters of batch digestion

	$P1$ $(LCH_4\ kg\ SV^{-1})$	Specific methane potential $(LCH_4\ kg\ SV^{-1})$	$Pmax$ $(LCH_4\ kg\ SV^{-1})$	R_{max} $(LCH_4\ kg\ SV^{-1}d^{-1})$	λ (d)	R^2
Orange peels batch digestion						
Op	14.71±3.92	103±5	90.94±2.36	10.89±0.21	16.80±0.33	0.9907
Op 10 Biochar	18.63±2.63	209±10	196.87±2.95	14.27±0.28	9.76±0.19	0.9909
Op 30 Biochar	29.04±4.29	298±15	280.99±4.21	14.15±0.28	9.32±0.18	0.9910
Sewage sludge batch digestion						
SS	7.75±2.76	273±14	271.15±4.06	18.73±0.37	7.91±0.15	0.9970
SS 10 Biochar	4.00±1.70	364±18	367.95±5.51	23.13±0.46	5.23±0.10	0.9990
SS 30 Biochar	16.22±3.05	425±21	412.96±6.19	33.39±0.66	5.89±0.11	0.9980
Orange peels and sewage sludge batch codigestion						
Op+SS	12.81±2.15	298±15	298.73±4.48	14.35±0.28	7.29±0.14	0.9956
Op+SS 10 Biochar	0	500±28	501.92±25.40	66.34±1.15	3.55±0.15	0.9950
Op+SS 30 Biochar	0	704±36	704.10±32.10	75.53±3.20	3.25±0.12	0.9954

753 P_1 is the initial methane production obtained, Pmax is the maximum methane yield, R_{max} is the

754 maximum methane production rate and λ is the lag–phase time

755

756 **Table 3.** Main parameters of particle size analysis applied after sludge digestion

Samples	Mean µm	Median µm	Mode µm	SSA cm² mL⁻¹	d10 µm	d50 µm	d90 µm
Biochar							
SS	29.9	19.2	21.7	5869	4.94	19.2	62.4
SS 10 Biochar	29.6	19.6	26.1	7818	3.65	19.6	57.1
SS 30 Biochar	21.2	16.3	26.1	8634	3.37	16.3	43.3

757 **Table 4.** Main parameters of semicontinuous digestion of orange peels and sewage sludge

Parameters	RC_Op+SS				RB_Op+SS			
HRT (days)	30	25	20	10	30	25	20	10
Evaluation period (days)	60	10	44	15	60	10	44	15
Specific methane production ($L\ CH_4\ kg\ VS^{-1}$)	318±73	288±39	338±70	268±42	512±120	491±82	393±80	254±23
Methane content (%)	56.0±0.5	56.0±0.5	57.0±0.5	64.0±0.5	56.0±0.5	56.0±0.5	57.0±0.5	59.0±0.5
H_2S content (ppm)	100±2	85±1	44±1	52±1	90±1	54±1	27±1	46±1
Ammonia ($g\ L^{-1}$)	1.63±0.19	1.75±0.87	1.38±0.14	1.78±0.14	1.55±0.16	1.71±0.72	1.37±0.17	1.75±0.10
pH	7.64±0.10	7.59±0.10	7.32±0.10	7.12±0.10	7.69±0.10	7.59±0.10	7.31±0.10	7.21±0.10
Total organic carbon soluble ($g\ L^{-1}$)	0.24±0.12	0.49±0.20	0.40±0.14	0.95±0.30	0.24±0.12	0.48±0.22	0.40±0.14	0.80±0.22
Total solid ($g\ L^{-1}$)	23.2±2.4	21.0±3.1	22.3±3.1	36.3±4.8	25.6±6.6	25.5±3.9	29. ±3.3	37.3±2.6
Volatile solid ($g\ L^{-1}$)	14.4±0.1	14.4±0.1	16.4±3.2	30.4±4.8	16.8±3.9	18.1±3.7	22.9±2.1	28.6±2.3
Volatile Solid feed (g)	4.5±0.2	5.4±0.3	6.7±0.3	13.4±0.6	4.5±0.2	5.4±0.3	6.7±0.3	13.4±0.7
Volatile solid removal (%)	67±2	67±3	63±7	32±10	62±8	60±8	49±6	36±8

Figure Captions

Fig. 1 Cumulative methane production and Gompertz adjustment curve: orange peels (Op) (a), sewage sludge (SS) (b) and codigestion systems (Op+SS) (c)

Fig. 2 Parameters measured during batch digestion of orange peels (Op) and with biochar addition at 10 g L^{-1} (Op 10 Biochar) and 30 g L^{-1} (Op 30 Biochar): limonene (a), total polyphenols (b) and volatile fatty acids (acetic, propionic and butyric acid) (c)

Fig. 3 Heat maps and hierarchical cluster at the family level, of the archaeal (a), and of the eubacterial community samples (b). The histogram shows the relative abundance of each family within a sample
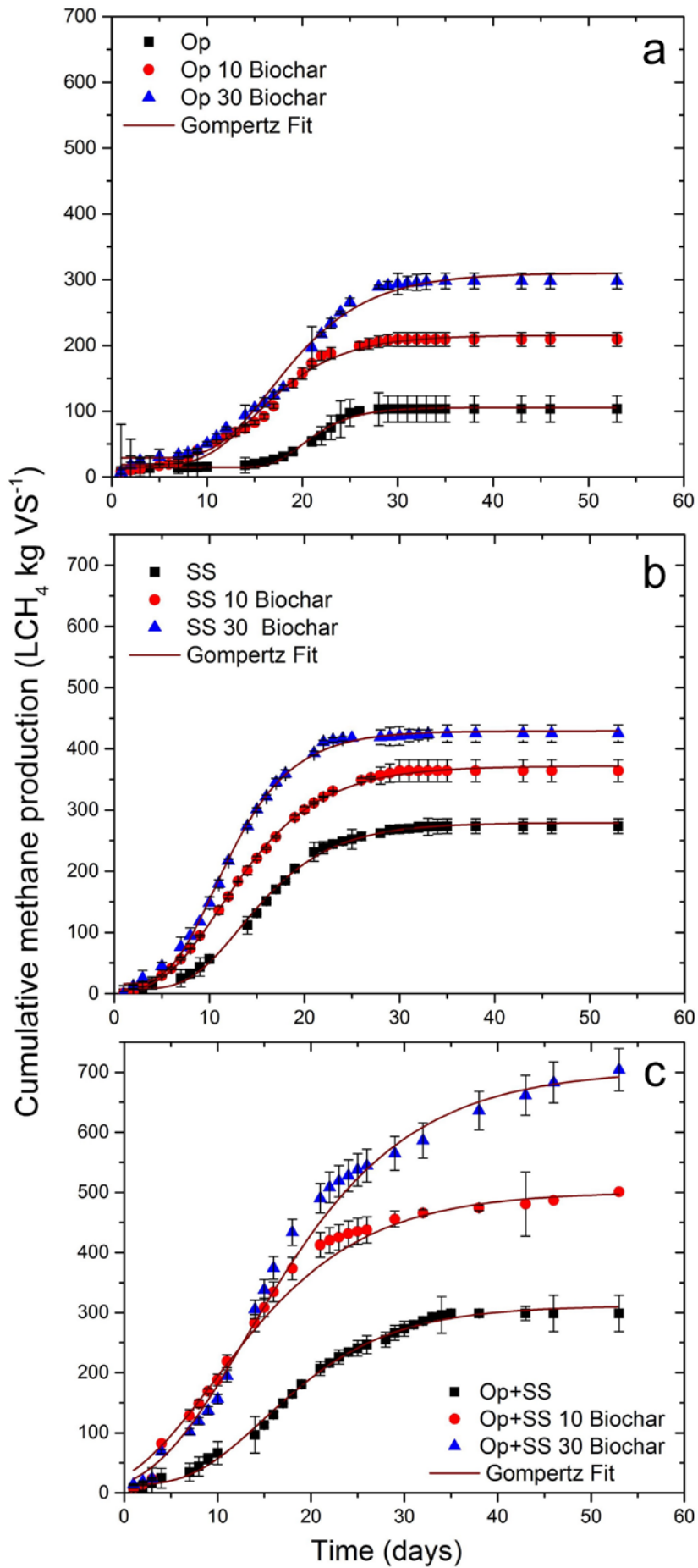
Fig. 4 Taxonomic classification at genus level for eubacterial (a) and archaeal (b) community of orange peels digestion. Groups making up less than 1% of the total number of sequences per sample were classified as "others"
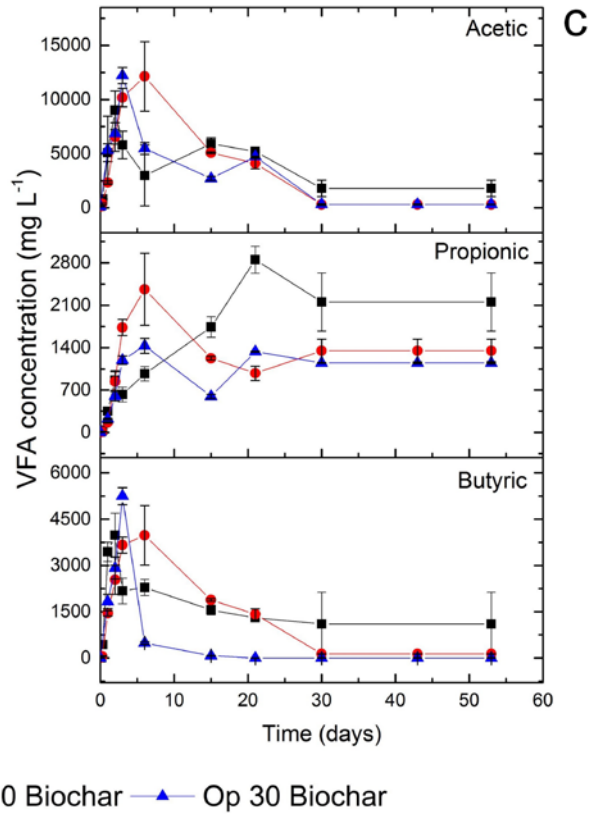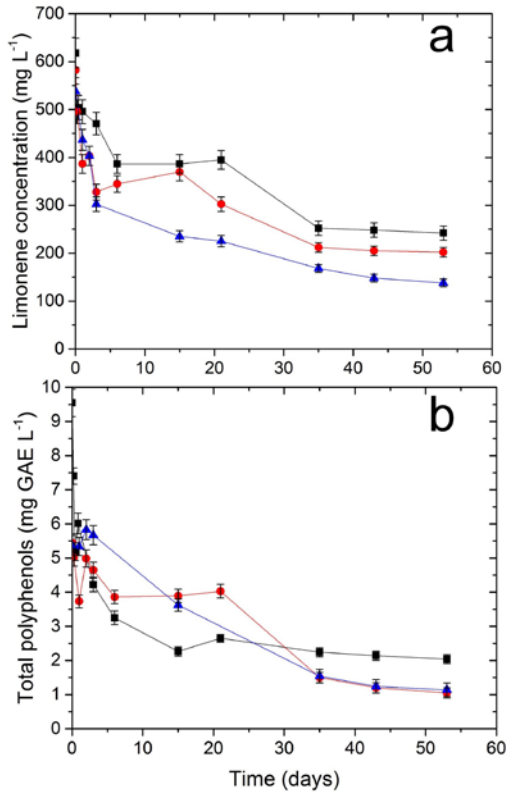
Fig. 5 Taxonomic classification at genus level for eubacterial (a) and archaeal (b) community of sewage sludge digestion. Groups making up less than 1% of the total number of sequences per sample were classified as "others"

Fig. 6 Parameters measured during semicontinuous digestion of orange peels and sewage sludge: Specific methane production (a), biochar concentration (b), limonene (c), total polyphenols (d) and total volatile fatty acids (acetic, propionic and butyric acid) (e)

For any of the figures not color is required in printed version

All graphs were created in Origin pro2015